Pharm Res (2014) 31:706–719
DOI 10.1007/s11095-013-1192-3

RESEARCH PAPER

A Novel Rapamycin-Polymer Conjugate Based on a New Poly(Ethylene Glycol) Multiblock Copolymer

Wanyi Tai • Zhijin Chen • Ashutosh Barve • Zhonghua Peng • Kun Cheng

Received: 13 June 2013 / Accepted: 9 August 2013 / Published online: 26 September 2013

ABSTRACT

Purpose Rapamycin has demonstrated potent anti-tumor activity in preclinical and clinical studies. However, the clinical development of its formulations was hampered due to its poor solubility and undesirable distribution *in vivo*. Chemical modification of rapamycin presents an opportunity for overcoming the obstacles and improving its therapeutic index. The objective of this study is to develop a drug-polymer conjugate to increase the solubility and cellular uptake of rapamycin.

Methods We developed the rapamycin-polymer conjugate using a novel, linear, poly(ethylene glycol) (PEG) based multiblock copolymer. Cytotoxicity and cellular uptake of the rapamycin-polymer conjugate were evaluated in various cancer cells.

Results The rapamycin-polymer conjugate provides enhanced solubility in water compared with free rapamycin and shows profound activity against a panel of human cancer cell lines. The rapamycin-polymer conjugate also presents high drug loading capacity (wt% ~ 26%) when GlyGlyGly is used as a linker. Cellular uptake of the conjugate was confirmed by confocal microscopic examination of PC-3 cells that were cultured in the presence of FITC-labled polymer (FITC-polymer).

Conclusion This study suggests that the rapamycin-polymer conjugate is a novel anti-cancer agent that may provide an attractive strategy for treatment of a wide variety of tumors.

KEY WORDS multiblock copolymer · PEG · polymer-drug conjugate · rapalogue · rapamcyin

W. Tai · Z. Chen · A. Barve · K. Cheng (✉)
Division of Pharmaceutical Sciences, School of Pharmacy
University of Missouri-Kansas City, 2464 Charlotte Street
Kansas City, Missouri 64108, USA
e-mail: chengkun@umkc.edu

Z. Peng
Department of Chemistry, University of Missouri-Kansas City
5100 Rockhill Road Kansas City, Missouri 64110, USA

ABBREVIATIONS

FKBP12	FK-binding protein 12
mTOR	The mammalian target of rapamycin
PEG	Poly(ethylene glycol)
Rapalogues	Rapamycin analogues
RBCs	Red blood cells

INTRODUCTION

Rapamycin, also known as sirolimus, is a carboxylic macrolide compound that was originally discovered as the product of a bacteria from soil sample of island Rapa Nui in the South Pacific (1). It was first developed as an antifungal drug by Ayerst Research Laboratories, but the potent immunosuppressive and anti-proliferative effects were discovered later (2). Rapamycin was approved as an immunosuppressive agent by the US Food and Drug Administration (FDA) in 1999. Due to its unique cytostatic effect, rapamycin has also entered into clinical trials to treat various cancers, including breast cancer, prostate cancer and glioblastoma (3–5). The molecular mechanism of rapamycin is to inhibit the mammalian target of rapamycin (mTOR) signaling pathway by directly binding to FK-binding protein 12 (FKBP12) and mTOR1. Because of the importance of the mTOR signal pathway in cancer development, rapamcyin was found to be active against almost all types of solid tumors (2). Rapamycin exhibits an exquisite selectivity to mTOR and demonstrates potent anti-tumor activity in the nanomolar range *in vitro*. Besides inhibiting cancer cell proliferation, rapamycin can also induce tumor endothelial cell death and vessel thrombosis by acting as a vascular AKT/mTOR inhibitor, which facilitates its anti-tumor effect (6,7).

Although rapamycin has broad and potent anti-tumor activity, it is insoluble in water and possesses poor distribution *in vivo*, which dramatically limits its clinical application

(8–10). Structurally, rapamycin does not contain any acidic or basic group that can increase aqueous solubility by salt formation (8,11). As a result, rapamycin is very hydrophobic and the solubility in water is only about 33 μg/mL (2.6 μg/mL in some reports) (12). Moreover, it is very difficult to prepare injectable rapamycin formulations for preclinical/clinical studies because rapamycin is only slightly soluble in many cosolvents such as ethanol, PEG 400 and polysorbate 80 (8). Rapamycin also exhibits a poor distribution profile *in vivo*. Due to the ubiquitous presence of the FK-binding proteins (high affinity to rapamycin) in red blood cells (RBCs), rapamycin exhibits a preferential distribution in RBCs. As reported by Yatscoff *et al.*, 95% of rapamycin in the blood is distributed in RBCs compared to 3.1% in the plasma, 1.0% in lymphocytes and 1.0% in granulocytes (9). Because RBCs can protect rapamycin from hepatic metabolism and renal filtration, rapamycin exhibits a relatively long terminal half-life (61–72 h in humans) compared with other small molecules (13). However, low partition in the plasma dramatically hinders the diffusion of rapamycin from the blood into tumor cells. In addition, it was reported that rapamycin was extensively distributed among many tissues in rats (tissue to blood partition coefficient Kp>40 in some cases) because of its lipophilic nature (14). The extensive distribution of rapamcyin in tissues is believed to account for its high apparent distribution volume (5.6–17.6 L/kg) and toxic effects (15,16).

To overcome these limitations, rapamycin has been chemically modified to hydrophilic analogues, such as CCI-779, RAD001 and AP23573 (Fig. 1a) (17). CCI-779, also known as Temsirolimus (Torisel, Wyeth), is an ester prodrug of rapamycin for treatment of renal cell carcinoma. By introducing 2,2-bis(hydroxylmethyl) propionic ester at the 42-OH of rapamycin, CCI-779 increases its hydrophilicity and makes the analogue readily soluble for intravenous formulation (18). RAD001, also known as Everolimus (Afinitor, Novartis), is a hydroxyl-ethyl ether of rapamycin with improved aqueous

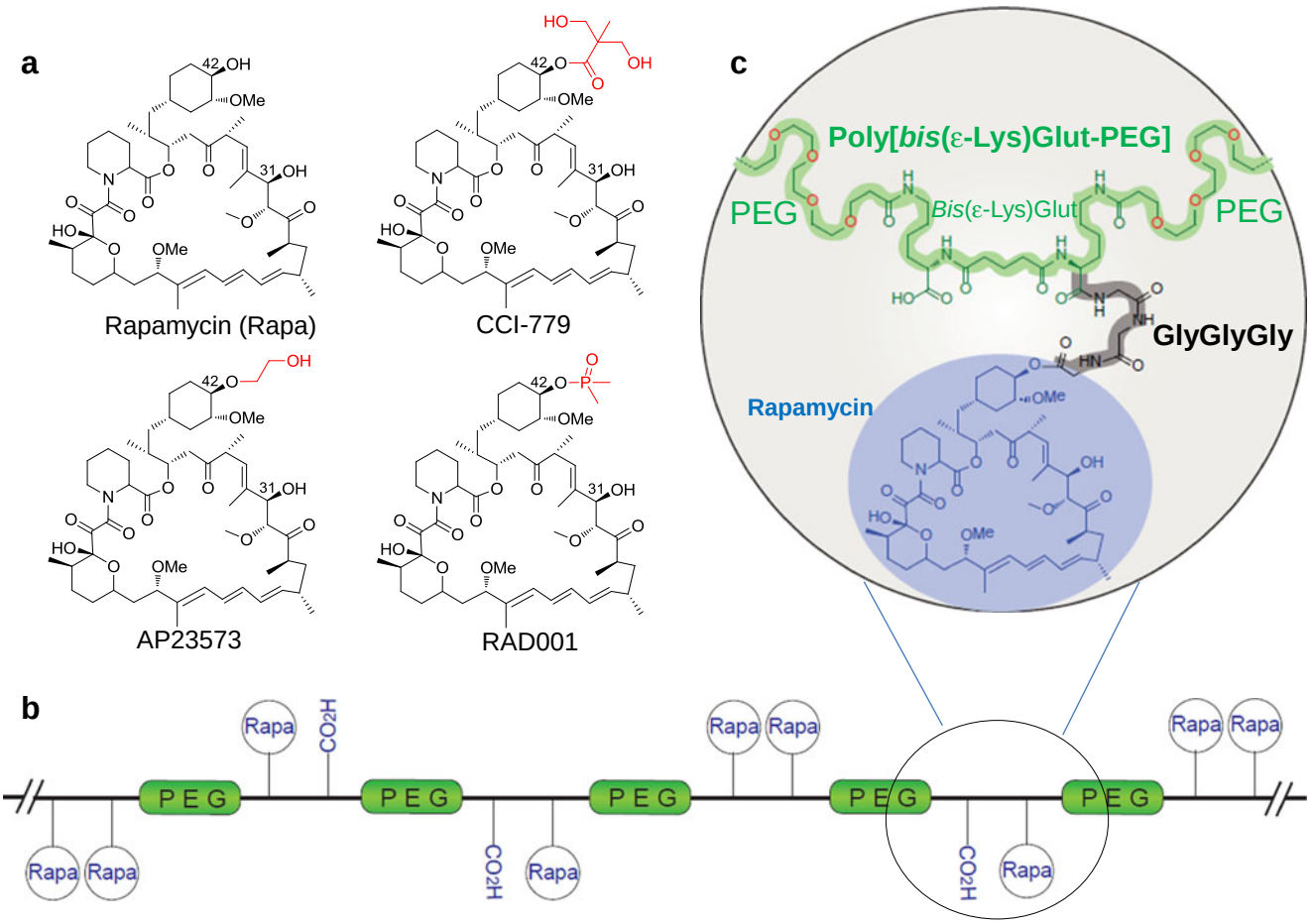

Fig. 1 Engineering of the rapamycin-polymer conjugate. (**a**) Structural comparison of rapamycin and rapalogues (CCI-779, AP23573 and RAD001). All of them are chemically modified at 42-OH position which is believed to minimally compromise their bioactivities. (**b**) The schematic graph illustrating the architecture of rapamycin-polymer conjugate **8c**. Instead of small molecular-weight moieties (highlighted in red in rapalogues structure), rapamycin in **8c** is conjugated to high molecular-weight polymer which can dramatically change its solubility and biodistribution profile. Rapamycin (Rapa) is uniformly distributed throughout the multiblock copolymer. The drug molecules are separated from each other by PEG to avoid aggregation; (**c**) The representative chemical structure of one block of the polymer-drug conjugate.

solubility and oral absorption (19). AP23573 (Deforolimus, Merck/Ariad) is a novel non-prodrug rapamycin analogue in which 42-OH is conjugated with a phosphate group to increase aqueous solubility and oral bioavailability (20). However, these rapamycin analogues (rapalogues) still have limited aqueous solubility (CCI-779: 0.12 mg/mL; RAD001: 0.1 mg/mL; AP23573: < 1 mg/mL) (15). Cosolvent such as ethanol is always required for intravenous formulation (21). Moreover, it was reported that the rapalogue CCI-779 can be quickly hydrolyzed into rapamycin by plasma esterase and subsequently redistributed into RBCs. Although other two rapalogues, RAD001 and AP23573, cannot be converted into rapamycin *in vivo*, moderate binding to RBCs was still observed in preclinical studies (22). Therefore, it is necessary to explore other rapamycin conjugates to improve aqueous solubility and tissue distribution profile, especially to minimize the distribution to RBCs.

Compared to the chemical modification, direct conjugation of rapamycin to a polymer may offer a better approach to overcome its limitations. Many hydrophobic drugs, such as paclitaxel and camptothecin, have demonstrated excellent aqueous solubility and pharamcokinetics after being conjugated to hydrophilic polymers (23–26). However, rapamycin is sensitive to light, temperature and pH, which make it hard to tolerate many chemical reactions. Although rapamycin has been successfully conjugated with wortmanin and other small molecules under mild reaction conditions, little attempt has been made to conjugate it with macromolecules, such as polymers and antibodies (27–29). In this study, we developed a novel, water-soluble, poly(ethylene glycol) (PEG) based multiblock copolymer for rapamycin conjugation. To conjugate rapamycin with the polymer, a tri-peptide linker GlyGlyGly was conjugated with rapamycin at 42-OH and then grafted onto the pendant carboxylic groups in polymer chains. The rapamycin-polymer conjugate exhibits excellent solubility in water and potent anti-tumor activity, suggesting its promising potential for clinical development.

MATERIALS AND METHODS

Materials

All reagents listed below were obtained from commercial sources and used without further purification. Rapamycin was purchased from LC laboratories (Woburn, MA). NHS-PEG_{3400}-NHS was purchased from Nanocs Inc. (New York, NJ). 2-(7-Aza-1H-benzotriazole-1-yl)-1,1,3,3-tetramethyluronium hexafluorophosphate (HATU) and N-Hydroxybenzotriazole (HOBT) were ordered from Genscript Inc. (Piscataway, NJ). Thiazolyl Blue was obtained from RPI Corp. (Prospect, IL). Fmoc-Lys(Boc)-OH and Trt-Gly-OH were purchased from Chem-Impex International Inc. (Wood Dale, IL). TO-PRO-3 stain was obtained from Life Technologies (Grand Island, NY). All solvents, including anhydrous solvents, HPLC grade solvents and other common organic solvents were purchased from commercial suppliers and used without further purification.

Cell Culture

All the cell lines used in this study were obtained from ATCC. LNCaP, PC-3, MCF-7, MCF-7/HER2 and SK-BR-3 cells were grown in RPMI-1640 medium containing 10% Fetal Bovine Serum (FBS), 100 units/mL penicillin, and 100 μg/mL streptomycin. HeLa and DU145 cells were cultured in DMEM medium supplemented with 10% FBS and 100 units/mL penicillin-100 μg/mL streptomycin mixtures. All the cells were grown at 37°C in a humidified atmosphere with 5% CO_2. Media were changed every other day, and the cells were passaged when they reached 80–90% confluency.

Synthesis of Bis(ε-amino-*L*-Lysine Benzyl ester) Glutaric amide, bis(ε-Lys-OBn)Glut, 5

The synthesis of comonomer *bis*(ε-Lys-OBn)Glut **5** was started from Fmoc-Lys(Boc)-OH. Fmoc-Lys(Boc)-OH was first esterified with benzyl alcohol, followed by removing Fmoc group by 20% piperidine-DCM according to Agnihotri's report (30). One gram of NH_2-Lys(Boc)-OBn **3** was dissolved in 50 mL of dry DCM, and then Glutaric acid (0.16 g) and EDCI (0.57 g) were added to the solution. The coupling reaction was initialized by adding 0.52 mL of triethylamine (Et_3N) to the solution. After stirring overnight at room temperature, the reaction was stopped with 50 mL of saturated NH_4Cl aqueous solution. The organic layer was separated, dried with Na_2SO_4, and concentrated under vacuum. The compound **4** was purified from the pale white residue by silica gel chromatography ($CHCl_3$/MeOH = 50/1, v/v). To remove the Boc groups, compound **4** (0.5 g) was dissolved in 30 mL of TFA/DCM (v/v, 1/1) and stirred at room temperature for 1 h. The solvent was evaporated under vacuum, and ice-cold diethyl ether was added to precipitate the product. The white precipitate was collected by filtration and dried under vacuum to get the pure product **5** (~ 60%). ^{1}H NMR (400 MHz, D_2O) δ 7.27 (s, 5H), 5.05 (m, 2H), 4.25 (t, 1H), 2.79 (t, 2H), 1.95 (m, 2H), 1.65 (m, 3H), 1.53 (m, 2H), 1.26 (m, 2H). ESI-MS calcd. for $C_{31}H_{44}N_4O_6$ 568.7; found 569.3 $(M + H)^{1+}$.

Synthesis of Poly[bis(ε-Lys-OBn)Glut-PEG], 6a-d

Before the reaction, *bis*(ε-Lys-OBn)Glut **5** was dried in a vacuum desiccator for 2 days. *Bis*(ε-Lys-OBn)Glut **5** (19 mg) and NHS-PEG_{3400}-NHS (100 mg) were transferred to a dry 5-mL flask, followed by adding 0.5 mL of extra dry DMF

(water < 50 ppm). The solution was stirred at room temperature for 10 min, and then anhydrous Et_3N was added into the reaction in nitrogen atmosphere. After stirring at room temperature or 50°C for 2–24 h, the mixture was diluted with 50 mL of water and dialyzed against distilled water using a dialysis tubing with MWCO 14,000. The polymer solution was lyophilized, and pure polymer **6a-d** was collected as white powder (60–80%). The molecular weight of polymer was determined on a Tosoh EcoSec HLC 8320GPC system equipped with a differential refractometer. The gel permeation column (Styragel®, 8 μm 300×7.5 mm, Waters Corporation) was calibrated using polystyrene standards and eluted with THF at a flow rate of 0.7 mL/min. As for **6b**, Mw= 31.5 kDa, Mn=21.9 kDa, Mw/Mn=1.43. ^{1}H NMR (400 MHz, D_2O) δ 7.30 (s, 5H), 5.08 (m, 2H), 4.26 (t, 1H), 4.07 (m, 2H), 3.61 (m, PEG-CH_2), 3.43 (m, 2H), 2.95 (m, 2H), 2.16 (m, 2H), 2.15–2.18 (m, 5H), 1.35 (m, 2H).

Synthesis of Linker-Drug, Gly-Rapa and GlyGlyGly-Rapa

*31-O-TMS Rapamycin **10***. 31-Trimethylsilyl Rapamycin was synthesized according to the procedure described by Shaw and Nan (31,32). Briefly, Rapamycin (200 mg) and imidazole (150 mg) were dissolved in 25 mL of DCM. After cooling to 0°C, trimethylsilyl chloride (TMSCl) solution in DCM (1 M, 1.3 mL) was slowly added into the reaction. The reaction was stirred for around 10 min at 0°C. After the reaction was complete, the mixture was directly applied on silica gel column and eluted with petroleum ether/acetone (v/v, 5/1). The purified intermediate 31,42-*bis*-O-TMS Rapamycin **9** (210 mg) was then dissolved in 20 mL of DCM, followed by adding 100 mg of imidazole/imidazole·HCl (mole ratio, 1/1). After stirring at room temperature for 3 h, the reaction was stopped and 31-O-TMS Rapamycin **10** was purified by flash chromatography on silica gel (petroleum ether/acetone, v/v= 5/1). The overall yield for the two-step reaction is ~ 50%. ^{1}H NMR (400 MHz, $CDCl_3$) δ 6.41 (m, 2H), 6.17 (q, 1H), 6.05 (d, 1H), 5.59 (q, 1H), 5.33 (d, 1H), 5.22 (d, 1H), 5.05 (q, 1H), 4.73 (s, 1H), 4.07 (d, 1H), 3.85 (m, 2H), 3.72 (m, 1H), 3.66 (d, 1H), 3.41 (s, 3H), 3.38 (m, 3H), 3.27 (s, 3H), 3.14 (s, 3H), 2.93 (m, 1H), 2.68 (m, 3H), 2.31 (m, 2H), 2.11 (m, 1H), 1.98 (m, 3H), 0.60–1.80 (m, 41H), 0.04 (s, 9H). ESI-MS calcd. for $C_{54}H_{87}NO_{13}Si$ 986.4; found 1008.7 $[M + Na]^+$.

*Trt-Gly-Rapa **12***. 31-O-TMS Rapamycin **10** (100 mg) and Trt-Gly-OH (64 mg) were dissolved in 5 mL of DCM. After stirring at room temperature for 5 min, EDCI (40 mg) and DMAP (2 mg) were added to the reaction. The reaction mixture was continuously stirred for 2 h at room temperature. Trt-Gly-Rapa(31-O-TMS) **11** was purified from the reaction using silica gel chromatography (petroleum ether/acetone, v/v=5/1). The TMS group at the 31 site of **11** was removed using inorganic acid. Briefly, compound **11** was dissolved in 4 mL of ice-cold THF, followed by adding 2 mL of 2 N H_2SO_4 solution. The reaction was warmed to room temperature and stirred for 30 min. After the reaction was complete, the mixture was poured into 20 g of ice and neutralized by adding excess amount of $NaHCO_3$. The neutralized solution was extracted with AcOEt. The organic phase was washed with brine, dried and concentrated. The residue was applied on a silica gel column and purified using petroleum ether/acetone (v/v=3/1) as the elution solution (yield, ~ 80%). H NMR (400 MHz, $CDCl_3$) δ 7.46 (d, 6H), 7.28 (m, 6H), 7.26 (t, 3H), 6.36 (m, 2H), 6.13 (q, 1H), 5.95 (d, 1H), 5.55(q, 1H), 5.42 (d, 1H), 5.29 (d, 1H), 5.15(q, 1H), 4.79 (s, 1H), 4.61 (m, 1H), 4.17 (d, 1H), 3.87 (m, 1H), 3.75 (d, 1H), 3.66 (m, 1H), 3.55 (d, 1H), 3.38 (m, 1H), 3.33 (s, 3H), 3.30 (s, 3H), 3.27 (m, 1H), 3.14 (s, 3H), 3.08 (m, 1H), 2.69 (m, 2H), 2.58 (m, 1H), 2.32 (m, 2H), 2.17 (s, 2H), 2.05 (m, 1H), 1.93 (m, 3H), 0.75–1.80 (m, 41H). ESI-MS calcd. for $C_{71}H_{98}N_2O_{13}$ 1213.5; found 1213.7 $[M + H]^+$.

*Gly-Rapa **13***. Protecting group Trt was removed using 0.1 M HOBT in trifluoroethanol (TFE) as reported (33). Briefly, compound 12 (50 mg) was dissolved in 3 mL of freshly prepared 0.1 M anhydrous HOBT in TFE. The reaction was stirred at room temperature for 10 min. The process of the reaction was monitored by TLC. After the Trt group was completely removed, 100 mL of water was added to stop the reaction. The white suspension was then extracted with 100 mL of AcOEt. The organic phase was washed with brine, dried by Na_2SO_4 and concentrated under vacuum. Gly-Rapa **13** was purified from the residue using silica gel chromatography ($CHCl_3$/MeOH, v/v= 10/1) and yielded as white powder (~70%). H NMR (400 MHz, $CDCl_3$) δ 6.36 (m, 2H), 6.14 (q, 1H), 5.95 (d, 1H), 5.56(q, 1H), 5.43 (d, 1H), 5.28 (d, 1H), 5.16(q, 1H), 4.97 (s, 1H), 4.73 (m, 1H), 4.18 (d, 1H), 3.86 (m, 1H), 3.75 (d, 1H), 3.66 (m, 1H), 3.55 (d, 1H), 3.43 (m, 2H), 3.37 (s, 3H), 3.33 (s, 3H), 3.14 (s, 3H), 2.81 (m, 1H), 2.69 (m, 2H), 2.59 (m, 1H), 2.32 (m, 2H), 2.12 (s, 1H), 2.04 (m, 2H), 1.99 (m, 3H), 0.75–1.80 (m, 45H). ESI-MS calcd. for $C_{53}H_{82}N_2O_{14}$ 971.2; found 971.9 $[M + H]^+$.

*GlyGlyGly-Rapa **15***. Compound **13** (20 mg) and Trt-GlyGly-OH (20 mg) were dissolved in 10 mL of dry DCM. After stirring at room temperature for 5 min, EDCI (10 mg) and Et_3N (8 μL) were added to the mixture. After 2 h, the reaction was stopped by adding 10 mL of saturated NH_4Cl aqueous solution. The organic phase was then separated, washed with brine, dried by Na_2SO_4 and concentrated under vacuum. The intermediate Trt-GlyGlyGly-Rapa **14** was purified on silica gel column ($CHCl_3$/MeOH, v/v=50/2.5). The Trt group of **14** was deprotected using the same method as described above. The final product GlyGlyGly-Rapa **15** was purified by silica gel chromatography ($CHCl_3$/MeOH, v/v=5/1, then 2/1). The yield for the two steps was 50 ~ 60%. ^{1}H NMR (400 MHz, $CDCl_3$) δ 6.35 (m, 2H), 6.13 (q, 1H),

6.00 (d, 1H), 5.51(q, 1H), 5.41 (d, 1H), 5.27 (d, 1H), 5.14(q, 1H), 4.66 (m, 2H), 4.23 (d, 1H), 4.01 (m, 4H), 3.89 (m, 2H), 3.65 (m, 2H), 3.57 (d, 1H), 3.31–3.35 (m, 4H), 3.14 (s, 3H), 2.96 (s, 3H), 2.89 (s, 3H), 2.62 (m, 1H), 2.31 (m, 2H), 0.75–2.00 (m, 53H). ESI-MS calcd. for $C_{57}H_{88}N_4O_{16}$ 1085.3; found 1085.8 $[M + H]^+$.

Synthesis of Rapamycin-Polymer Conjugate

Synthesis of Poly[bis(ε-Lys)Glut–PEG] **7**. Polymer **7** was synthesized by removing the benzyl groups from carboxylic acids of polymer **6b** *via* hydrogenation. Briefly, polymer **6b** (150 mg) was dissolved in 50 mL of methanol in nitrogen atmosphere. Twenty milligrams of Pd/C (palladium loading 10%) was transferred into the reaction flask under nitrogen atmosphere. After all the Pd/C was merged into methanol, nitrogen was changed into hydrogen, and the reaction was stirred at room temperature overnight. The reaction mixture was then filtered to remove Pd/C. The filtrate was concentrated and dried under vacuum overnight to get polymer **7** in quantitative yield. ^{1}H NMR (400 MHz, D_2O) δ 4.20 (m, 1H), 4.10 (m, 2H), 3.61 (m, PEG-CH_2), 3.43 (m, 2H), 3.01 (t, 2H), 2.21 (t, 2H), 1.82 (m, 1H), 1.69 (m, 1H), 1.55 (m, 2H), 1.41 9 m, 2H), 1.25 (m, 2H).

Synthesis of Rapamycin-Polymer Conjugate 8a-c. Conjugate **8a-c** was synthesized by coupling linker-drugs (rapamycin, Gly-Rapa and GlyGlyGly-Rapa) with polymer **7** using EDCI/Et_3N/NHS. Briefly, polymer **7** (5 mg, 0.0015 mmol of repeat unit) and linker-drug (0.006 mmol) were dissolved in 0.5 mL of dry DMF. EDCI (10 mg), DMAP (2 mg) and NHS (1 mg) were added into the reaction and stirred for 24 h. The polymer was then precipitated with diethyl ether (20 mL). After centrifugation, ether was poured out and the precipitate was dissolved in 5 mL of water. The insoluble solid was removed by filtering through 0.2 μm filters. The solution was dialyzed against distilled water by 14 kDa MWCO membrane at room temperature for 48 h. Dialysis water was changed every 8 h. The solution was free-dried to yield as a white solid (yield, 41–88%).

Synthesis of Rapamycin-Polymer Conjugate 8d. Conjugate 8d was synthesized using the same method as described above but the coupling reagent was changed to HATU/DIPEA. Briefly, polymer **7** (5 mg) and GlyGlyGly-Rapa **15** (6 mg) were added into 0.5 mL of dry DMF, followed by HATU (20 mg) and DIPEA (16 μL). The reaction was continuously stirred at room temperature for 24 h. Twenty milliliter of diethyl ether was poured into the reaction to precipitate the product. The precipitate was collected by centrifugation (4,000 g, 5 min) and re-dissolved in 5 mL of water. After dialysis and free drying, the pure conjugate **8d** yielded as a light brown powder (yield ~ 50%).

Determination of Rapamycin Loading Efficacy (wt%)

The percentage of rapamycin conjugated to polymers (wt%) was determined by Ultraviolet–visible (UV) spectrophotometry. The standard curve was generated with a series of rapamycin solution in water (λ_{max}=280 nm). The polymer-drug conjugates were diluted in water, and the UV absorbance at 280 nm was measured. Rapamycin concentration was calculated from the standard curve. The percentage of rapamycin conjugated to polymer (wt%) was calculated by dividing the amount of rapamycin by the total weight of the polymer-drug conjugate.

Rapamycin Release from the Polymer Conjugates

Aliquots of GlyGlyGly-Rapa and rapamycin-polymer conjugate **8c** stock solution (10 mM in DMSO) were diluted to 200 μM in water. The solutions were immediately mixed with 100% human/rat/mouse sera, which gave a final concentration of 100 μM rapamycin in 50% sera. Forty microliters of the solution were divided into 0.2 mL Eppendorf tubes and incubated at 37°C. At selected time intervals, serum proteins were precipitated with 120 μL of acetonitrile plus 0.1% TFA. After centrifugingation at 12,000 g for 10 min, 100 μL of the supernatant was collected and analyzed with HPLC for quantification of the released rapamycin.

The HPLC system was equipped with a Shimadzu LC-20AT pump, a SIL-10AF auto-sampler and a SPD-10A UV detector. The separation was achieved on a Waters C18 column (250 mm×4.6 mm, 5 μm) at a flow rate of 1.0 mL/min. The mobile phases were consisted of phase A (water, 0.1% formic acid) and B (acetonitrile, 0.1% formic acid), with a gradual increase of phase B from 50–90% over 20 min. The absorbance of rapamcyin was monitored at 280 nm.

In Vitro Cytotoxicity

In vitro cytotoxcity of rapamycin, the polymer and rapamycin-polymer conjugates was determined according to the method we reported before (34). Briefly, cells were seeded into 96-well plates at a density of 5,000 cells/well. Twenty-four hours after incubation, a series of drug dilutions ranging from 0.001 to 1000 nM were added to the wells and cultured for another 72 h. The relative cell numbers were measured using MTT assay. To enhance the assay sensitivity, twenty-five microliters of Sorensen's glycine buffer (0.1 M glycine, 0.1 M NaCl, adjust pH to 10.5 with 0.1 N NaOH) was added into wells according to a previous report (35). The absorbance was measured using a DTX 880 Multimode Detector (Beckman Coulter,Inc., Fullerton, CA) at the wavelength of 570 nm. IC_{50} was calculated by fitting a concentration – absorbance curve using Graphpad Prism 5 (Graphpad software Inc, La Jolla, CA).

Cellular Uptake Analysis by Confocal Laser Scanning Microscopy

Cellular uptake of the FITC-labeled polymer was performed and analyzed by confocal laser scanning microscopy as reported (36). Briefly, PC-3 cells were seeded into 8-well Lab-Tek^{TM} chamber slides (Nunc Inc. Rochester, NY) and cultured for 24 h. The culture medium was discarded, and monolayers were washed once with RPMI-1640 medium. Polymer-FITC was diluted to 10 μM in RPMI-1640 and added into the chambers. After incubation for 24 h, the cells were washed six times with DPBS and fixed in 4% buffered formalin at room temperature for 10 min. The cells were washed three times to remove remaining formalin, and the nucleus was stained with TO-PRO-3 (Excitation/Emission: 642/661 nm) according to manufacturer's protocol (Invitrogen, Grand Island, NY). After washing, cell monolayers were mounted onto glass microscope slides using fluorescence mounting medium (Vector Lab, Burlingame, CA). The cellular uptake and distribution was analyzed using Nikon C1 laser scanning confocal microscope (Nikon Instrument Inc., Melville, NY).

Aqueous Solubility Assay

The aqueous solubilities of rapamycin and its conjugates were assayed by the thermodynamic method as reported before (34). Briefly, excess amount of rapamycin or its conjugates were suspended in 100 μL of distilled water. The suspension was shaken at room temperature for 24 h. The suspension was then centrifuged at 12,000 g for 15 min to remove undissolved drug. The supernatant was collected, and the concentration was quantified by UV spectrometry at 280 nm.

Statistical Analysis

Data were expressed as the mean ± standard deviation (SD). Difference between any two groups was determined by ANOVA. $P<0.05$ was considered statistically significant.

RESULTS

Novel Engineering of Rapamycin-Polymer Conjugate

In prior studies, rapamycin was specifically conjugated with small molecular-weight moieties to increase its hydrophilicity and specificity (CCI-779, APA23573 and RAD001, Fig. 1a). Although the oral bioavailability was enhanced, the solubility and biodistribution profile were only slightly improved. In this paper, a rapamycin-polymer conjugate was engineered by conjugating rapamycin with a novel, PEG based, multiblock copolymer. The architecture of the polymer is composed of alternating PEG and *bis*(ε-Lys)Glut units. Each *bis*(ε-Lys)Glut unit is grafted by one or two rapamycin (Rapa) molecules and separated from other *bis*(ε-Lys)Glut unit by PEG (Fig. 1b and c). Therefore, drugs are evenly distributed along the polymer chain and all the drugs are well separated from each other by PEG. Compared to the drug position patterns in other polymer-drug conjugates (polyaspartice acid and polymerglutamic acid - drug conjugate), this unique architecture can dramatically reduce the heterogeneity and avoid aggregation (37). Moreover, this novel alternating, multiblock copolymer contains two drug conjugation sites in each block, which enables high drug loading capacity (wt%) (32.1% for rapamycin). Rapamycin is attached onto the polymer by tri-peptide GlyGlyGly linker which can dramatically increase drug loading efficiency. Rapamycin is linked with GlyGlyGly *via* a potentially cleavable ester linkage, which can be gradually released by enzymatic/chemical hydrolysis (Fig. 1c).

Synthesis of multiblock copolymers Poly [*bis*(ε-Lys-OBn)Glut-PEG], 6a-d, and Poly[*bis*(ε-Lys) Glut-PEG], 7

The multiblock copolymer Poly[*bis*(ε-Lys-OBn)Glut-PEG] was synthesized by condensation of monomer NHS-PEG_{3400}-NHS with comonomer *bis*(ε-Lys-OBn)Glut **5** in the presence of organic base. *Bis*(ε-Lys-OBn)Glut **5** is composed of one glutaric acid and two *L*-lysine linked at α-amino groups (Fig. 2). The ε-amino group of *L*-Lysine was less sterically hindered and more nucleophilic than the α-amino group, therefore making it more reactive to monomer NHS-PEG_{3400}-NHS. Comonomer *bis*(ε-Lys-OBn)Glut **5** was synthesized according to the scheme in Fig. 2. Compound **3** was synthesized from **1** according to Agnihotri's report (30). Glutaric acid was coupled with at least 2 equivalents of compound **3** using EDCI/DMAP. Compound **4** was carefully purified by silica gel flash chromatography and treated with TFA/DCM to get comonomer *bis*(ε-Lys-OBn)Glut **5**. Polymerization was carried out in anhydrous DMF in nitrogen atmosphere. After the polymerization was initialized by organic base Et_3N, the viscosity of the solution increased dramatically in less than 1 h. The reaction mixture became very viscous after 24 h, which indicated successful elongation of the polymer chain. As shown in Table I, polymerization at 50°C can produce higher Mw than that at 25°C. It might be because that high temperature can reduce the viscosity of the polymerization solution and therefore increase the condensation efficiency (38). Polymer Mw reduced to around 20 kDa when inorganic base $NaHCO_3$ was used. Although both Et_3N and $NaHCO_3$ can deprotonate the ε-amino groups of *bis*(ε-Lys-OBn)Glut **5**, $NaHCO_3$ is partially insoluble in DMF, making it less efficient in polymerization. Polymer **6a-d** are highly soluble in water, THF and chloroform, but insoluble in diethyl ether and petroleum ether.

To graft rapamycin onto polymer, polymer **6b** was deprotected by hydrogenation to liberate the carboxyl groups

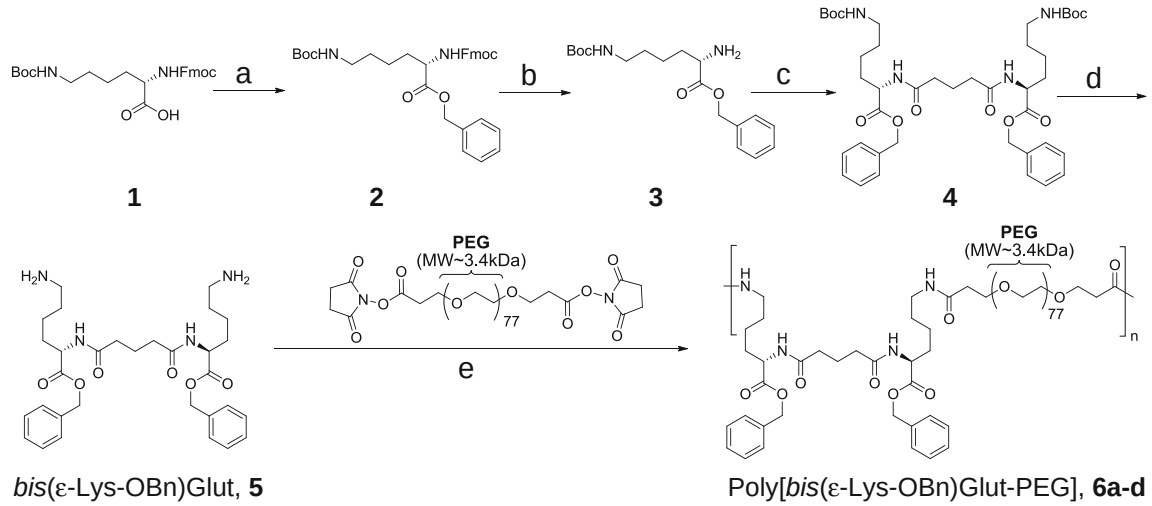

Fig. 2 Synthesis of Poly[*bis*(ε-Lys-OBn)Glut-PEG]. Reagents and conditions: (**a**) Benzyl alcohol, EDCI, DMAP; (**b**) 20% piperidine in DCM; (**c**) Glutaric acid, EDCI, DMAP; (**d**) TFA/DCM, rt; (**e**) Et_3N, DMF.

(Fig. 3). Polymer **7** is a novel, linear multiblock copolymer containing two carboxyl groups for drug conjugation in each block. This polymer is also soluble in water, DMF, and methanol, slightly soluble in $CHCl_3$, but insoluble in THF and diethyl ether.

Synthesis of the Rapamycin-Polymer Conjugate

Rapamycin was first conjugated with polymer **7** by forming an ester bond between its hydroxyl groups and polymer's carboxyl groups in the presence of EDCI, Et_3N and NHS. Conjugate **8a** was purified by dialysis with a yield around 67%. However, conjugate **8a** had very low drug loading capacity (wt% ~ 0.48%). If all the carboxyl groups were conjugated with rapamycin, the theoretical maximal drug loading capacity (wt%) could be as high as 34.1%. Therefore, the hydroxyl group of rapamycin only reacted with around 1.4% of all the carboxyl groups in polymer **7**. The low coupling efficiency could be explained partially by the steric hindrance between the polymer and rapamycin. To reduce the steric hindrance, two linkers, Gly and GlyGlyGly, were utilized to link polymer **7** and rapamycin.

Linker-drugs were synthesized according to the scheme in Fig. 4. In order to selectively conjugate the linkers at 42-OH, 31-OH of rapamycin was selectively protected with TMS group according to the procedure described by Shaw and Nan (31,32). Trt-Gly-OH was then conjugated with 42-OH using a conventional coupling method. After removing TMS at 31-OH in diluted inorganic acid H_2SO_4, Trt-Gly-Rapa was deprotected with 0.1 M HOBT in TFE to get Gly-Rapa **13**. Routine Trt deprotection methods, such as 1% TFA in DCM, were inapplicable because rapamycin is very sensitive to TFA. Gly-Rapa **13** was further coupled with Trt-Gly-Gly-OH using EDCI/Et_3N to give compound **14**. GlyGlyGly-Rapa **15** was finally obtained by removing the Trt group from compound **14**.

Linker-drugs Gly-Rapa **13** and GlyGlyGly-Rapa **15** were conjugated with polymer **7** using the same coupling method as the synthesis of **8a**. Conjugate **8b** was obtained with a yield of 65–88%, and the weight percentage (wt%) of rapamycin in the polymer-drug conjugate was 19.5%. The highest weight percentage of rapamycin in polymer-drug conjugates was observed in conjugate **8c** (wt% ~ 27.3%) where around 80% of carboxyl groups in polymer 7 were conjugated with rapamycin. There was no significant difference in drug loading capacity when other coupling methods, such as HATU/DIPEA, were used (conjugate **8d**, Table II). Therefore, the conjugation efficiency is mainly determined by linkers rather than coupling methods.

Table I Polymerization of the Monomer NHS-PEG_{3400}-NHS with Comonomer *bis*(ε-Lys-OBn)Glut in Different Conditions

Polymer	Base	Temperature	Reaction lime	Mw (kDa)	Mn (kDa)	Mw/Mn	Yield (%)
6a	Et_3N	50°C	2 h	20.9	15.2	1.37	71
6b	Et_3N	50°C	24 h	31.5	21.9	1.43	59
6c	Et_3N	25°C	24 h	22.8	16.1	1.41	66
6d	$NaHCO_3$	50°C	24 h	19.9	14.1	1.42	79

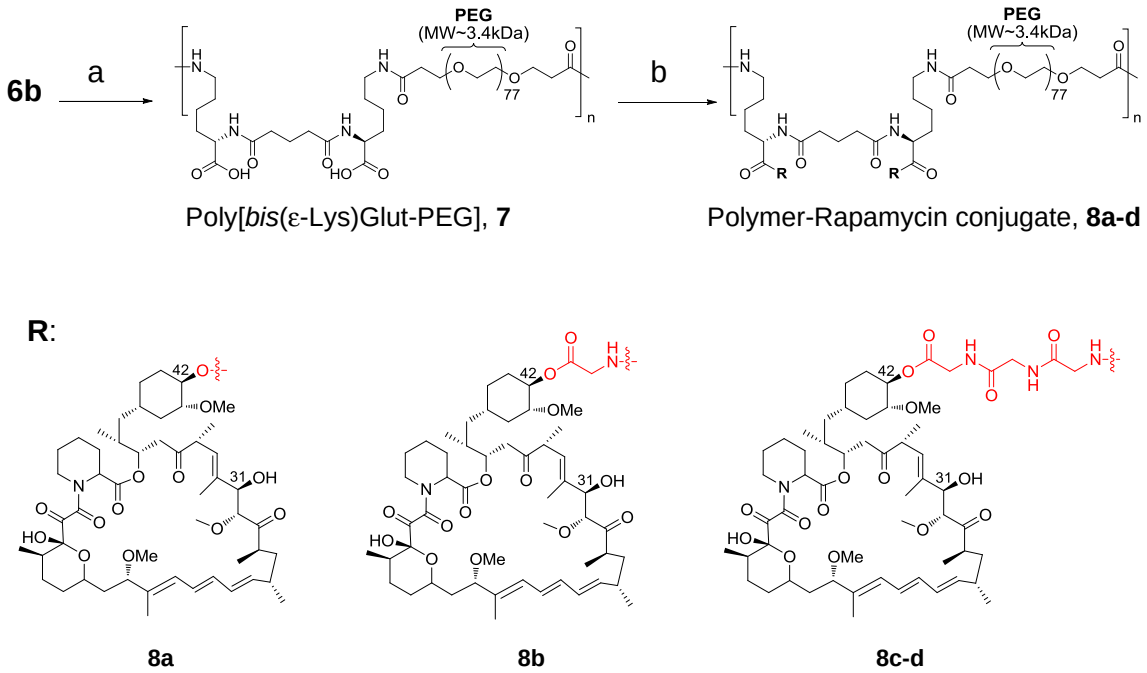

Fig. 3 Synthesis of the rapamycin-polymer conjugate. Reagents and conditions: (**a**) H_2, Pd/C in methanol; (**b**) EDCI, Et_3N, NHS.

Characterization of Rapamycin-Polymer Conjugate

The UV spectrum of conjugate **8c** was scanned over the range of 190 to 400 nm and compared with free rapamycin. As shown in Fig. 5, The UV spectrum of rapamycin exhibits a maximum absorbance peak at 280 nm and two small peaks on either side. Similar peaks were also observed in the UV spectrum of purified conjugate **8c**, which indicates that rapamycin is conjugated to the polymer chains. Besides three peaks around 280 nm, conjugate **8c** also shows strong absorbance at near ultraviolet region (200–230 nm), which is contributed mainly by polymer 7 and minimally by rapamycin (Fig. 5). The carboxyl groups in polymer 7 and double bonds in rapamycin are believed to be responsible for the UV absorbance at 200 ~ 230 nm.

Proton NMR (^{1}H NMR) spectroscopy was also determined to prove the presence of rapamycin in the rapamycin-polymer conjugate **8c**. Figure 6a shows the ^{1}H NMR spectrum of rapamycin. The seven groups of peaks (a - g) at low field

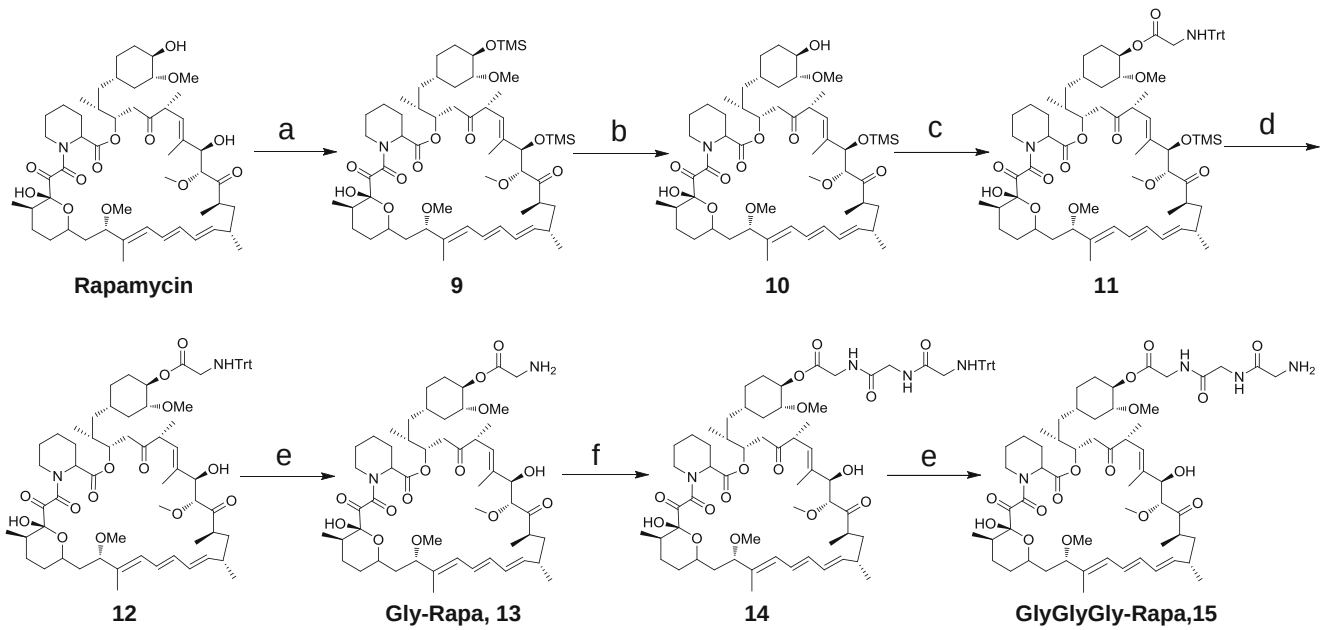

Fig. 4 Synthesis of GlyGlyGly-Rapa. Reagents and conditions: (**a**) TMSCl, imidazole, DCM; (**b**) imidazole/imidazole·HCl, DCM; (**c**) Trt-Gly-OH, EDCI, DMAP, DCM; (**d**) THF/2 N H_2SO_4 (v/v = 2/1); (**e**) 0.1 M HOBT in TFE; (**f**) Trt-Gly-Gly-OH, EDCI, Et_3N, DCM.

Table II Properties of the Rapamycin-Polymer Conjugates

Polymer-drug conjugate	Conjugation reagents	Linker-drug	Theoretical maximal drug conjugated (wt%)	Drug conjugated (wt%)	Yield (%)
8a	EDCI/Et_3N/NHS	Rapamycin	34.1	0.68 ± 0.18	57 ~ 71
8b	EDCI/Et_3N/NHS	Gly-Rapa	33.4	19.5 ± 1.8	65 ~ 88
8c	EDCI/Et_3N/NHS	GlyGlyGly-Rapa	32.1	27.3 ± 5.1	41 ~ 63
8d	HATU/DIPEA	GlyGlyGly-Rapa	32.1	24.9 ± 3.1	50 ~ 64

corresponds very well to the protons of double bonds (a–e) and carbonyl groups (f, g) in rapamycin. The single peaks (h–j), between 3.0 and 3.5 ppm, corresponds to the presence of three CH_3O- groups in rapamycin. The ^1H NMR spectrum of rapamycin-polymer conjugate **8c** (Fig. 6c) contains peaks representing both rapamycin and the polymer chain. Peaks a - j in Fig. 6c show the same chemical shifts (ppm) and splitting patterns as that in Fig. 6a, indicating the presence of rapamycin in the conjugate **8c**. While the polymer chain in the conjugate 8c corresponds to the peaks a' - c', in which peaks a' - b' represent *bis*(ε-Lys)Glut and peak c' represents PEG_{3400} (Fig. 6b).

Release of Rapamycin from Rapamycin Conjugates

The release of rapamycin from two conjugates GlyGlyGly-Rapa and conjugate **8c** was evaluated in mouse, rat and mouse serum. Rapamycin conjugates were incubated with 50% of different serum at 37°C for 4 h. The release profile of rapamycin was monitored using HPLC. In mouse serum, the half-life of releasing rapamycin from GlyGlyGly-Rapa is approximately 0.5 h. In contrast, the half-life increases to 4 h in rat serum. A minimal release was observed in human serum where only 10% of rapamycin was released after 4 h (Fig. 7). The species-dependent release profile is due to the metabolic differences between species (39). The similar phenomenon was also observed in Wortmannin-Rapamycin conjugate (27). The release of rapamycin from rapamycin-polymer conjugate **8c** is much slower than that of GlyGlyGly-Rapa. After 4-h incubation, only

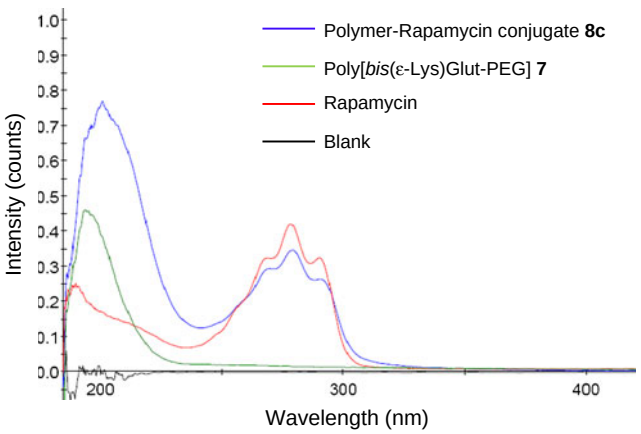

Fig. 5 UV spectra of rapamycin, rapamycin-polymer conjugate 8c and polymer 7.

~20%, ~ 9% and ~3% of rapamycin were released from conjugate **8c** in mouse, rat and human serum, respectively. The bulky polymer structure in polymer-rapamycin conjugate dramatically increases the steric hindrance of the ester linker between rapamycin 42-OH and GlyGlyGly, which makes ester bond less accessible by esterase and therefore decreases the hydrolysis rate (40). In addition, the release of rapamycin from polymer-rapamycin reached its plateau at 1 h and 2 h in mouse and rat serum, respectively. These premature plateau-release profiles can be attributed to the instability of rapamycin in sera. The half-life of rapamycin in rat plasma has been reported to be only 2.2 h, and a shorter half-life would be expected in mouse plasma due to its higher metabolic rate (39,41). Therefore, the plateau was reached when the degradation rate of rapamycin was equal to its release rate.

In Vitro Activity of Rapamycin and its Conjugates

The *in vitro* cytotoxicity of polymer **7**, rapamycin, GlyGlyGly-Rapa and conjugate **8c** was determined in prostate, breast, and cervical cancer cell lines using a MTT assay. No obvious cytotoxicity (IC_{50} > 100 μM) was observed in polymer **7** treated cells, indicating that polymer **7** is not toxic to these cancer cell lines. Rapamycin showed potent *in vitro* cytotoxicity to all cancer cell lines (Table III). The IC_{50} values of rapamycin in all seven cancer cell lines ranged from 0.1 to 5.2 nM. Compared to breast cancer cell lines, prostate and cervical cancer cell lines were much more sensitive to rapamycin treatment. GlyGlyGly-Rapa was 2- to 36-fold less potent than rapamycin with the exception of MCF-7/HER2, in which similar potency was observed. Given the fact that GlyGlyGly-Rapa is an ester prodrug of rapamycin, and hydrolysis is required for its activity, it is reasonable that GlyGlyGly-Rapa shows lower potency than rapamycin. The IC_{50} values of conjugate **8c** are in a range of 25–50 nM. Although it is less potent than free rapamycin, conjugate **8c** still exhibits low nanomolar IC_{50} values against all cancer cell lines tested.

Cellular Uptake and Distribution of Rapamycin-Polymer Conjugates

FITC ethylenediamine (FITC-NH_2) was conjugated to polymer **7** using the same coupling method (EDCI/NEt_3/NHS) as conjugate **8a-c**. The weight percentage (wt%) of FITC in

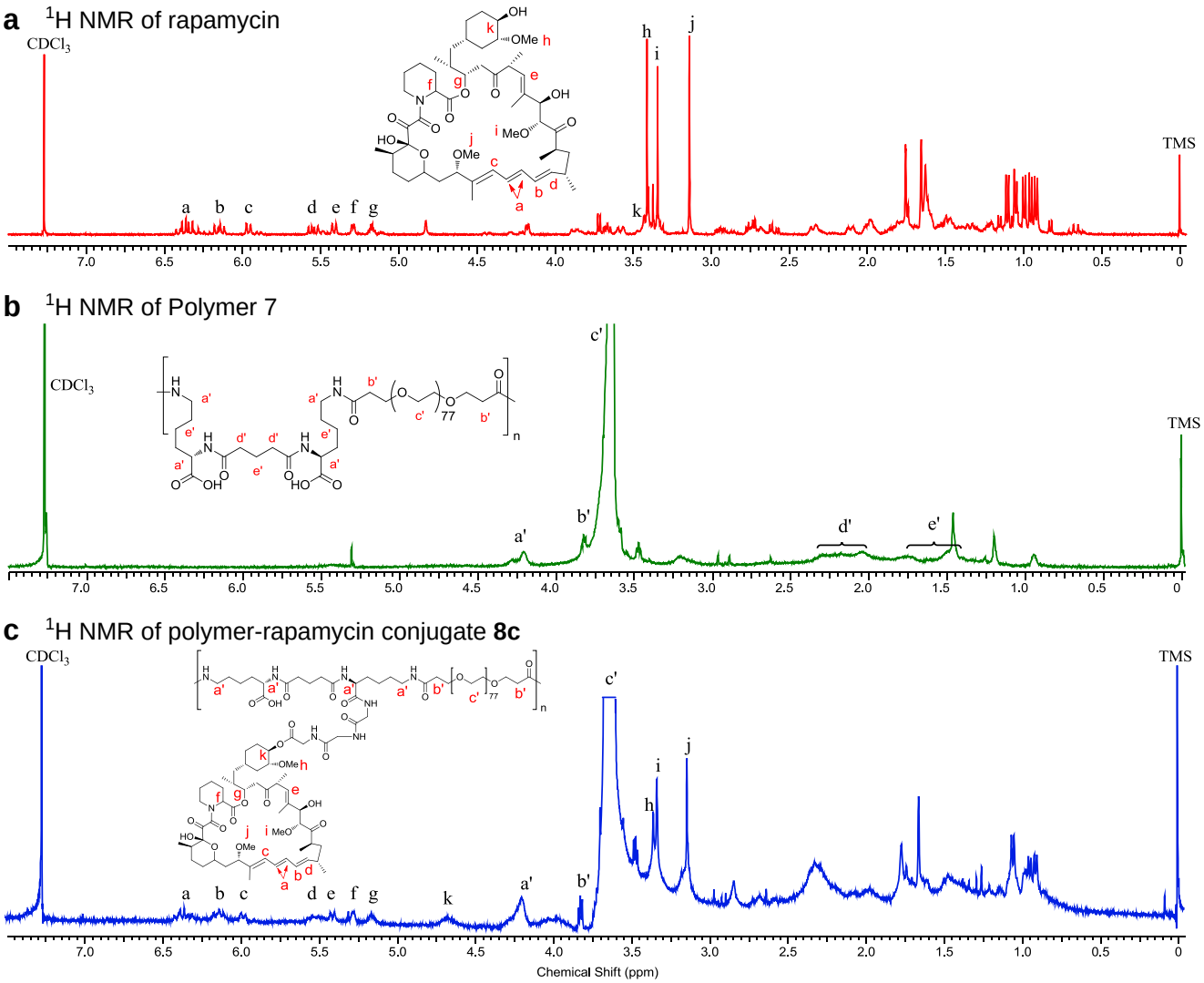

Fig. 6 ^{1}H NMR spectra of rapamycin (**a**), polymer 7 (**b**) and rapamycin-polymer conjugate 8c (**c**) in $CDCl_3$ solvent.

the labeled polymer **7** is 4.5% (Data not shown). To determine the cellular uptake and distribution, the FITC-labeled polymer was incubated with PC-3 cells in serum-free medium for 24 h. Punctuated staining pattern was observed in PC-3 cells after 24-h treatment (Fig. 8). Other fluorescently labeled polymers, such as β-cyclodextrin polymer and PEG, were

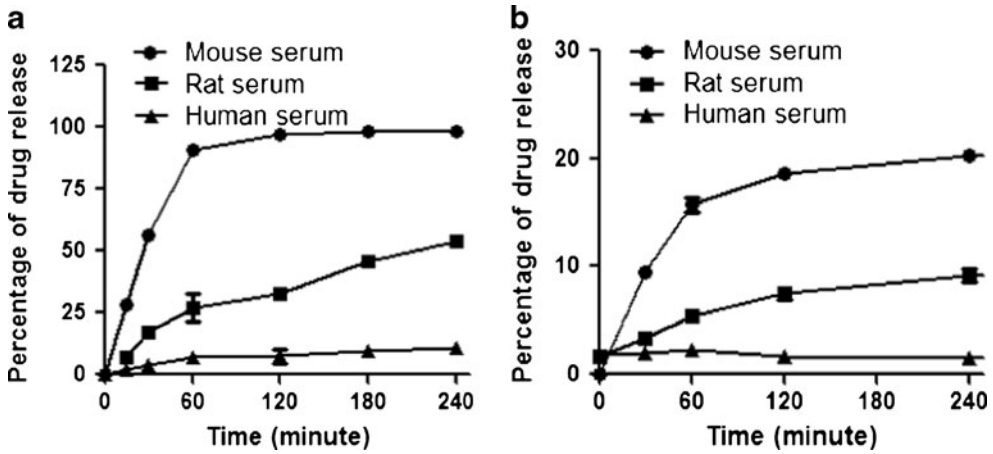

Fig. 7 The release profiles of rapamycin from GlyGlyGly-Rapa (**a**) and conjugate **8c** (**b**) in different sera.

Table III *In Vitro* Cytotoxicity (IC_{50}, nM). The Cancer Cells were Treated with the Compounds for 72 h Before MTT Assay. Values Shown are mean ± SD

Cancer type	Cell line	Polymer 7[a]	Rapamycin	GlyGlyGly-Rapa	Conjugate 8c[b]
Prostate	LNCaP	>100,000	0.9 ± 0.9	4.1 ± 0.3	51.2 ± 0.6
	PC-3	>100,000	0.8 ± 0.7	2.3 ± 0.6	29.9 ± 0.7
	DU145	>100,000	0.1 ± 0.5	5.6 ± 0.5	30.6 ± 0.6
Breast	SK-BR-3	>100,000	4.4 ± 0.3	9.2 ± 0.6	40.7 ± 0.7
	MCF-7	>100,000	5.2 ± 0.3	10.3 ± 0.5	26.3 ± 0.4
	MCF-7/HER2	>100,000	3.3 ± 0.2	3.9 ± 0.4	25.9 ± 0.5
Cervical	HeLa	>100,000	1.0 ± 0.1	36.5 ± 0.1	47.4 ± 0.1

[a] IC_{50} is calculated based on molar concentration of repeated units

[b] IC_{50} of polymer rapamycin conjugate 8c is expressed in terms of rapamycin equivalents

reported to share the similar cellular uptake and distribution pattern (36,42). Polymers are believed to enter cells *via* endocytosis because the punctated vesicular distribution of fluorescence indicated a lysosomal localization. The uptake of FITC-NH_2 in PC-3 cells was also examined. Because FITC-NH_2 is a membrane non-permeable fluorescent dye, no fluorescence was observed even after 24-h incubation (Fig. 8) (43).

Conjugation with Polymer Dramatically Enhanced the Solubility of Rapamcyin

Due to the hydrophilic PEG component, polymer **7** is highly soluble in water (Table IV). The aqueous solubility of rapamycin is only around 0.034 mg/mL at room temperature. After conjugated to polymer **7**, its solubility increases to 21.061 mg/mL which is more than 600 times higher than free rapamycin. The aqueous solubility of the rapamycin-polymer conjugate **8c** is around 78 mg/mL.

Table IV Aqueous Solubility of Polymer 7, Rapamycin and Conjugate **8c**

Compound	Aqueous solubility (mg/mL)	Aqueous solubility (Rapamycin equivalents)	
		mg/mL	mM
Polymer 7	100.332 ± 22.278	−/−	−/−
Rapamycin	0.034 ± 0.006	0.034 ± 0.006	0.037 ± 0.007
Conjugate 8c	78.000 ± 12.165	21.061 ± 3.285	23.014 ± 3.594

DISCUSSION

Rapamycin has been examined alone or in combination with other drugs for treatment of various cancers in clinical studies (3–5). Although it has shown promising therapeutic effects, its clinical development was interrupted by poor aqueous solubility and preferential distribution in RBCs. Various formulations and conjugates, such as cosolvent system, polymeric micellar formulation and some rapalogues, have been developed to overcome the limitations (8,15,17). All these approaches can only partially increase the solubility, but has little effect on the blood distribution and pharmacokinetics. Therefore, the objective of this study is to develop a rapamycin-polymer conjugate that not only enhance the solubility but also improve the biodistribution profiles of rapamycin.

In this study, rapamycin was conjugated with a novel, linear, PEG containing multiblock copolymer. The polymer was synthesized *via* the condensation of a difunctionalized PEG monomer (NHS-PEG_{3400}-NHS) with a comonomer

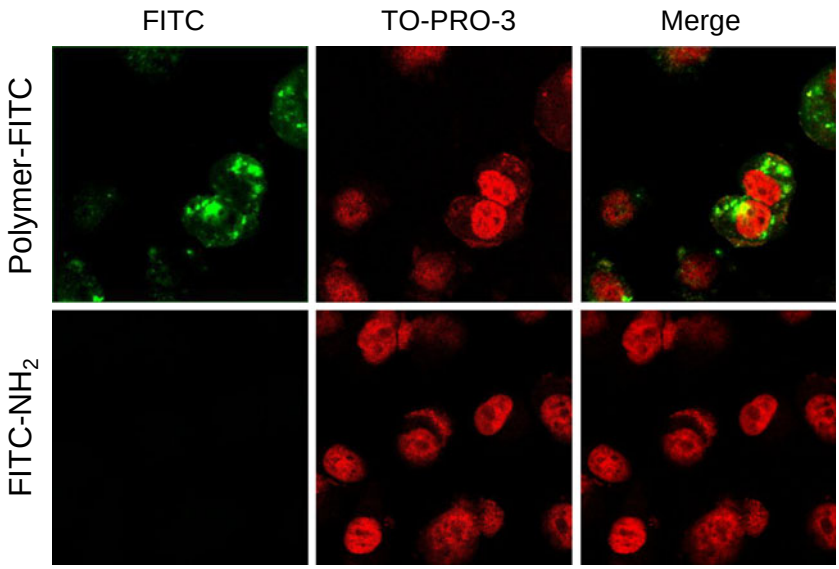

Fig. 8 Cellular uptake of FITC labeled polymer (Polymer-FITC) and FITC ethylenediamine (FITC-NH_2) by confocal microscopy. PC-3 cells were treated with Polymer-FITC and FITC-NH_2 in serum free RPMC-1640 media for 24 h. Cell nucleus was stained with TO-PRO-3 and imaged in two fluorescent channels.

bis(ε-Lys-OBn)Glut **5** containing two pendant carboxyl groups for drug conjugation. Comonomer *bis*(ε-Lys-OBn)Glut **5** is small in size and symmetric in structure, which is expected to enhance the condensation efficiency. The purity of the comonomer has a significant impact on achieving high M_W polymers. The presence of impurities can terminate the chain elongation, leading to low MW polymers (26). After precipitation in diethyl ether twice, *bis*(ε-Lys-OBn)Glut was obtained with a purity of ~ 97%. Beside impurity, moisture can also dramatically decrease the M_W of the polymer. Polymerization in non-drying solvent or with non-drying comonomer would only generate short polymer chains with M_W of ~18 kDa (data not shown).

This study represents the first attempt to conjugate rapamycin with a polymer. Rapamycin is a structurally complicated natural product which contains three hydroxyl groups. Although the tertiary alcohol at position 13 is highly hindered and unreactive, rapamycin contains two secondary hydroxyl groups at position 31 and 42 which are accessible for esterification and etherification. Directly reacting with acrylating agents would produce a mixture of 31,42-*bis*-acrylated product and 31- or 42-monoacrylated products, which results in inevitable heterogeneity of the rapamycin-polymer conjugate. In this study, we achieved the regioselective conjugation of rapamycin at 42-OH by first protecting the 31-OH with TMS and then synthesizing 42-monoacrylated rapamycin *via* esterification. Another challenge of rapamycin conjugation is its instability in both acidic and basic conditions which make it intolerable to many chemical reactions. Gly-Rapa was firstly attempted to synthesize from Fmoc-Gly-Rapa, but rapamycin was quickly degraded when deprotecting Fmoc in 10% piperidine in DCM. Removing Boc from Boc-Gly-Rapa was also problematic due to its sensitivity to TFA (even 1% TFA in DCM). Gly-Rapa was finally obtained with a very low yield (~ 10%) from Trt-Gly-Rapa by deprotecting Trt in THF/2 N H_2SO_4 (v/v=2/1, overnight). However, the yield was dramatically increased to 60~80% when the deprotection method was switched to an uncommonly used, but mild condition (0.1 N HOBT in TFE, 10 min).

Conjugation of rapamycin to the polymer was achieved by coupling a linker to rapamycin at position 42-OH, and subsequently grafting the linker-Rapa at the pendant carboxyl groups of this multiblock copolymer. The expected mechanism of drug release from the rapamycin-polymer conjugate is that tumor esterase would hydrolyze the 42-ester bond and release free rapamycin from the polymer backbone. Insertion of linkers, such as Gly or GlyGlyGly, between rapamycin and the polymer backbone is believed to accelerate the drug release (25,26,37). Moreover, these amino acids or peptide linkers can transform the hydroxyl group of rapamycin at position 42 to a more reactive amino end group, which could dramatically increase the drug loading capacity. As shown in Table II, directly conjugating rapamycin to the polymer can only load a small amount of drug (wt% ~ 0.68). In contrast, the drug loading capacities increased to 19.5% and 27.3%, respectively, by inserting Gly and GlyGlyGly between rapamcyin and the polymer. The use of longer linker, such as GlyGlyGly, resulted in a higher drug loading capacity because the long and flexible linker may reduce the steric hindrance between the polymer and rapamycin during coupling reaction. The resulting polymer rapamycin conjugate **8c** dissolves freely in water. Its aqueous solution is stable and does not precipitate/change color in the absence of strong ionic strength and light.

The most striking observation of this study is the great solubility of rapamycin after conjugating with the polymer. Rapamycin is practically insoluble in water (0.034 mg/mL), but its solubility increases to 21.061 mg/mL after conjugating with the polymer. This solubility meets the requirement for *i.v.* formulations in animal studies, in which the minimal dose concentration is 3~6 mg/mL, and clinical studies, in which the minimal dose concentration is 1 mg/mL (8). The backbone of polymer **7** contains repeating units of two components, PEG_{3400} and *bis*(ε-Lys)Glut, in which PEG_{3400} attributes to the aqueous solubility. Moreover, PEG_{3400} is also expected to reduce the toxicity and immunogenicity of the polymer (44). As shown in Table I, polymer **7** does not show obvious toxicity in various cultured tumor cells.

The release of rapamycin from the polymer-drug conjugate in the presence of serum was observed (Fig. 7). The polymer-rapamycin conjugate exhibits different release rates in the serum of different species, which indicates that the release of rapamycin is mainly mediated by enzymatic hydrolysis other than pure chemical hydrolysis. Bulk structure of the polymer dramatically hinders the enzymatic hydrolysis and therefore slowdowns the rapamycin release in the serum, which can avoid the redistribution of rapamycin into RBCs. Same to other polymer-drug conjugates, the rapamycin-polymer conjugate is taken up by tumor cells *via* the endocytotic pathway (Fig. 8) (36,42). In the intracellular compartment endosomes and lysosomes, rapamycin-polymer would be attacked by peptidase/esterase and release the drug rapamycin.

In conclusion, a novel, linear, PEG-based multiblock copolymer was synthesized and utilized as a carrier for hydrophobic drug rapamycin. The rapamycin-polymer conjugate shows significantly increased solubility in water and potent cytotoxicity against a panel of cancer cell lines. It also demonstrates that the polymer-drug conjugate can be taken up by tumor cells. The result of the uptake study indicates that the lysosome is the main site of the intracellular localization of the polymer-drug conjugate. Thus, in this study we reported a novel rapamycin conjugate which holds great promising for treatment of a wide variety of tumors.

ACKNOWLEDGMENTS AND DISCLOSURES

This project has been supported by two awards (R21CA143683 and R01AA021510) from the National Institute of Health (NIH). The authors gratefully acknowledge Lu Jin, Bin Qin and Ravi S. Shukla for helpful discussion and techical assistance.

REFERENCES

1. Vezina C, Kudelski A, Sehgal SN. Rapamycin (AY-22,989), a new antifungal antibiotic. I. Taxonomy of the producing streptomycete and isolation of the active principle. J Antibiot (Tokyo). 1975;28(10):721–6.
2. Garber K. Rapamycin's resurrection: a new way to target the cancer cell cycle. J Natl Cancer Inst. 2001;93(20):1517–9.
3. Zhao H, Cui K, Nie F, Jin G, Li F, Wu L, *et al*. Effects of rapamycin on Breast Cancer cell migration through the cross-talk of MAPK pathway. Cancer Res. 2009;69(24 suppl).
4. Armstrong AJ *et al*. A pharmacodynamic study of rapamycin in men with intermediate- to high-risk localized prostate cancer. Clin Cancer Res. 2010;16(11):3057–66.
5. Cloughesy TF *et al*. Antitumor activity of rapamycin in a Phase I trial for patients with recurrent PTEN-deficient glioblastoma. PLoS Med. 2008;5(1):e8.
6. Phung TL *et al*. Pathological angiogenesis is induced by sustained Akt signaling and inhibited by rapamycin. Cancer Cell. 2006;10(2):159–70.
7. Bruns CJ *et al*. Rapamycin-induced endothelial cell death and tumor vessel thrombosis potentiate cytotoxic therapy against pancreatic cancer. Clin Cancer Res. 2004;10(6):2109–19.
8. Simamora P, Alvarez JM, Yalkowsky SH. Solubilization of rapamycin. Int J Pharm. 2001;213(1–2):25–9.
9. Yatscoff R *et al*. Blood distribution of rapamycin. Transplantation. 1993;56(5):1202–6.
10. Ferron GM, Conway WD, Jusko WJ. Lipophilic benzamide and anilide derivatives as high-performance liquid chromatography internal standards: application to sirolimus (rapamycin) determination. J Chromatogr B Biomed Sci Appl. 1997;703(1–2):243–51.
11. Serajuddin AT. Salt formation to improve drug solubility. Adv Drug Deliv Rev. 2007;59(7):603–16.
12. Sun M *et al*. The influence of co-solvents on the stability and bioavailability of rapamycin formulated in self-microemulsifying drug delivery systems. Drug Dev Ind Pharm. 2011;37(8):986–94.
13. Gallant-Haidner HL *et al*. Pharmacokinetics and metabolism of sirolimus. Ther Drug Monit. 2000;22(1):31–5.
14. Napoli KL *et al*. Distribution of sirolimus in rat tissue. Clin Biochem. 1997;30(2):135–42.
15. Yanez JA *et al*. Pharmacometrics and delivery of novel nanoformulated PEG-b-poly(epsilon-caprolactone) micelles of rapamycin. Cancer Chemother Pharmacol. 2008;61(1):133–44.
16. Serkova N *et al*. Assessment of the mechanism of astrocyte swelling induced by the macrolide immunosuppressant sirolimus using multinuclear nuclear magnetic resonance spectroscopy. Chem Res Toxicol. 1997;10(12):1359–63.
17. Benjamin D *et al*. Rapamycin passes the torch: a new generation of mTOR inhibitors. Nat Rev Drug Discov. 2011;10(11):868–80.
18. Hidalgo M, Rowinsky EK. The rapamycin-sensitive signal transduction pathway as a target for cancer therapy. Oncogene. 2000;19(56):6680–6.
19. Goudar RK *et al*. Combination therapy of inhibitors of epidermal growth factor receptor/vascular endothelial growth factor receptor 2 (AEE788) and the mammalian target of rapamycin (RAD001) offers improved glioblastoma tumor growth inhibition. Mol Cancer Ther. 2005;4(1):101–12.
20. Fetterly GJ, Mita MM, Britten CD, Poplin E, Tap WD, Carmona A, *et al*. Pharmacokinetics of oral deforolimus (AP23573, MK-8669). 2008 ASCO Annual Meeting, 2008.
21. Rubino JTS, Siskavich V, Harrison MM, Gandhi P. Parenteral CCI-779 formulations containing cosolvents, an antioxidant, and a surfactant. US Patent. 2011;8026276.
22. Laplanche R, Meno-Tetang GM, Kawai R. Physiologically based pharmacokinetic (PBPK) modeling of everolimus (RAD001) in rats involving non-linear tissue uptake. J Pharmacokinet Pharmacodyn. 2007;34(3):373–400.
23. Li C *et al*. Complete regression of well-established tumors using a novel water-soluble poly(L-glutamic acid)-paclitaxel conjugate. Cancer Res. 1998;58(11):2404–9.
24. Li C *et al*. Biodistribution of paclitaxel and poly(L-glutamic acid)-paclitaxel conjugate in mice with ovarian OCa-1 tumor. Cancer Chemother Pharmacol. 2000;46(5):416–22.
25. Sapra P *et al*. Novel delivery of SN38 markedly inhibits tumor growth in xenografts, including a camptothecin-11-refractory model. Clin Cancer Res. 2008;14(6):1888–96.
26. Cheng J *et al*. Synthesis of linear, beta-cyclodextrin-based polymers and their camptothecin conjugates. Bioconjug Chem. 2003;14(5):1007–17.
27. Ayral-Kaloustian S *et al*. Hybrid inhibitors of phosphatidylinositol 3-kinase (PI3K) and the mammalian target of rapamycin (mTOR): design, synthesis, and superior antitumor activity of novel wortmannin-rapamycin conjugates. J Med Chem. 2010;53(1):452–9.
28. Umeda N *et al*. A photocleavable rapamycin conjugate for spatiotemporal control of small GTPase activity. J Am Chem Soc. 2011;133(1):12–4.
29. Naicker S, Sharma SK,Thomas W. Rapamycin peptides conjugates: synthesis and uses thereof. Patent. 2004. US Patent: 7659244.
30. Agnihotri G *et al*. Structure-activity relationships in nucleotide oligomerization domain 1 (Nod1) agonistic gamma-glutamyldiaminopimelic acid derivatives. J Med Chem. 2011;54(5):1490–510.
31. Shaw C-C, Sellstedt J, Noureldin R, Cheal GK, Fortier G. Regioselective synthesis of rapamycin derivatives. 2001. US Patent 6,277,983.
32. Fajun Nan JD, Zuo J, Yu L, Meng L, Zhang Y, Yang N, *et al*. Rapamycin carbonic ester analogues, pharmaceutical compositions, preparations and uses thereof. 2011. USPTO Applicaton No. 20110166172.
33. Bodanszky M, Bednarek MA, Bodanszky A. Coupling in the absence of tertiary amines. Int J Pept Protein Res. 1982;20(4):387–95.
34. Tai W *et al*. Development of a peptide-drug conjugate for prostate cancer therapy. Mol Pharm. 2011;8(3):901–12.
35. Plumb JA, Milroy R, Kaye SB. Effects of the pH dependence of 3-(4,5-dimethylthiazol-2-yl)-2,5-diphenyl-tetrazolium bromide-formazan absorption on chemosensitivity determined by a novel tetrazolium-based assay. Cancer Res. 1989;49(16):4435–40.
36. Cheng J, Khin KT, Davis ME. Antitumor activity of beta-cyclodextrin polymer-camptothecin conjugates. Mol Pharm. 2004;1(3):183–93.
37. Bhatt R *et al*. Synthesis and in vivo antitumor activity of poly(l-glutamic acid) conjugates of 20S-camptothecin. J Med Chem. 2003;46(1):190–3.
38. Liu C-Y *et al*. New linearized relation for the universal viscosity − temperature behavior of polymer melts. Macromolecules. 2006;39(25):8867–9.
39. Decarie A *et al*. Serum interspecies differences in metabolic pathways of bradykinin and [des-Arg9]BK: influence of enalaprilat. Am J Physiol. 1996;271(4 Pt 2):H1340–7.
40. Chandran SS *et al*. A prostate-specific antigen activated N-(2-hydroxypropyl) methacrylamide copolymer prodrug as dual-

targeted therapy for prostate cancer. Mol Cancer Ther. 2007;6(11):2928–37.
41. Ferron GM, Jusko WJ. Species differences in sirolimus stability in humans, rabbits, and rats. Drug Metab Dispos. 1998;26(1):83–4.
42. Murthy N *et al*. Design and synthesis of pH-responsive polymeric carriers that target uptake and enhance the intracellular delivery of oligonucleotides. J Control Release. 2003;89(3):365–74.
43. Sun Y *et al*. Intracellular labeling method for chip-based capillary electrophoresis fluorimetric single cell analysis using liposomes. J Chromatogr A. 2006;1135(1):109–14.
44. Veronese FM, Mero A. The impact of PEGylation on biological therapies. BioDrugs. 2008;22(5):315–29.